Phi: Jurnal Pendidikan Fisika dan Terapan
Vol. 12, No. 2 (2026) 384-396
ISSN: 2460-4348, e-ISSN: 2549-7162
https://jurnal.ar-raniry.ac.id/index.php/jurnalphi/index

Article Type: *original research*

Electrical Resistivity Imaging on Limestone Formation for Aquifers Identification in Poguwatu Village, Central Sumba

Aulia Nareswari[1*], Andri Yadi Paembonan[2], Acep Ruchimat[3]
[1,2]Geophysical Engineering, Sumatera Institute of Technology, South Lampung, Indonesia
[3] Center for Groundwater and Environmental Geology, Bandung, Indonesia

Correspondence E-mail: aulianareswari2004@gmail.com

ARTICLE INFO

Article History:
Received: 20 May 2026
Revised: 26 June 2026
Accepted: 27 July 2026
Published: 31 July 2026

Keywords:
Resistivity method, Aquifer, Dipole-Dipole;

ABSTRACT

Poguwatu Village in Central Sumba Regency is a dry area characterized by low rainfall and dominated by carbonate rocks, resulting in limited surface water availability and posing a persistent challenge for groundwater exploration. This study presents the first subsurface investigation using the Dipole-dipole resistivity geoelectrical method to characterize aquifer-bearing rock conducted in Poguwatu Village, West Cendana. This method has the ability to identify the conductor zone related to the saturation area where the water accumulated. Measurements were conducted along 5 survey lines, where each line has 620 m length, except Line 5 extending to 880 m, with 10 m electrode spacing. The measured data calculate in apparent resistivity value and then invert to true resistivity using least-square inversion processes. The result yielded RMS errors ranging from 17.7% to 24.8%. The inversion results identified four rock units based on resistivity values, sandy limestone saturated with saline water (< 2.0 Ωm), marl (2.0–32.0 Ωm), fractured or sandy limestone (32.0–128.0 Ωm), and compact limestone (>128.0 Ωm). A seepage with thickness ± 2 m was identified on Line 2 within the fractured/sandy limestone, bounded below by an impermeable marl. Compact limestone, with very low porosity and permeability, dominates in most of the study area and functions as an aquifuge, a finding corroborated by a dry borehole on Line 5 that failed to yield groundwater. These results indicate limited groundwater potential across Poguwatu Village, and further investigation into alternative water sources from surrounding areas is recommended for the community's water supply.

This work is licensed under a Creative Commons Attribution-ShareAlike 4.0 International License

1. INTRODUCTION

The community in Poguwatu Village, faces difficulties in accessing clean water due to prolonged dry seasons and limited surface water sources. The population in this area is predominantly employed in the agricultural, forestry, and fishery sectors (Badan Pusat Statistik Kabupaten Sumba Barat, 2025). Making access to clean water a fundamental necessity that sustains both daily life and economic activity. According to the Meteorology, Climatology, and Geophysics

Agency (BMKG), the average rainfall in Central Sumba, East Nusa Tenggara, generally falls within the low (0–50 mm) to moderate (51–150 mm) criteria (Badan Meteorologi, 2021).

Based on interviews with local residents, many wells exhibit a water level difference of more than 10 m between the dry and rainy seasons, and since these wells frequently dry up or experience a significant reduction in discharge during the dry season, they appear to be unsuitable as reliable aquifers (Inamoto & Sayama, 1993). This unpredictability occurs because karst aquifers are highly heterogeneous systems where groundwater flow is fundamentally driven by a combination of matrix porosity, fissures, and dissolution-enlarged conduits (Stevanović, 2019). These unpredictable conduit networks introduce significant geometric uncertainty regarding the subsurface flow paths, which poses persistent challenges for accurate subsurface and aquifer characterization (Hartmann & Baker, 2017; Torrese, 2020).

Nevertheless, groundwater remains an abundant and renewable resource, generally stored within the pore spaces of certain rock formations known as aquifers. Aquifer is highly dependent on the amount of rainfall as well as the local lithological and geological conditions (Multi et al., 2023). Geologically, Poguwatu Village is located within the Pamalar Formation (Tmp), characterized by limestone and claystone in its lower section, and the Waikabubak Formation (Tmpw), which consists of limestone, argillaceous limestone, and interbedded sandy marl and tuffaceous marl (**Figure 4.**) (Inamoto & Sayama, 1993; Krisnasiwi, 2021). The morphology of central Sumba, dominated by hilly and coastal terrain, combined with carbonate rocks of low porosity and permeability, makes groundwater difficult to encounter near the surface (Badan Pusat Statistik Kabupaten Sumba Barat, 2025). Based on **Figure 1.** the research location is underlain by Predominantly Reef Limestones, Alternating with Bedded Limestones, locally with intercalations of marly limestones and tuffs. In terms of groundwater potential, the study area falls within the locally extremely little water quantities zone (partly 0.1 l/s), although higher discharge rates (>5 l/s) remain possible in karst systems such as karst springs and underground rivers.

Carbonate rock dissolution depends on lithological factors, such as chemical and mineralogical purity of the rock, and physicochemical factors, such as temperature and CO_2 partial pressure (Hartmann et al., 2014). Mapping groundwater in highly carbonated environments using standard methods frequently fails due to the extreme resistivity contrasts between compact limestone to fractured/sandy limestone saturated with saline water. To investigate the subsurface conditions, the resistivity geoelectric method can be employed as an effective approach for identifying aquifer potential through variations in resistivity values. Electrical resistivity methods have gained significant popularity in groundwater investigations, also offer numerous advantages, such as their field-friendly nature, ability to provide subsurface information at depths ranging from a few meters to hundreds of meters, and the availability of software for 2D and 3D interpretation (Hussein et al., 2023). Among various arrays, the Dipole-Dipole configuration offers superior capability in delineating groundwater pathways within carbonate formations, due to its high sensitivity to lateral changes and sharp horizontal resistivity contrasts. (Firdaus et al., 2023).

Although previous regional studies, such as the groundwater potential assessment in East Sumba using satellite and geoelectric methods were conducted Prabawa et al., (2020). Investigations focusing on the local aquifer within Poguwatu Village, Central Sumba remain critically limited. Therefore, the novelty of this study lies in the application of 2D Electrical Resistivity Tomography (ERT) to identify potential aquifers, particularly within a predominantly limestone terrain. This study aims to provide a reliable hydrogeological model expected to accurately delineate productive clean water resources for the local community.

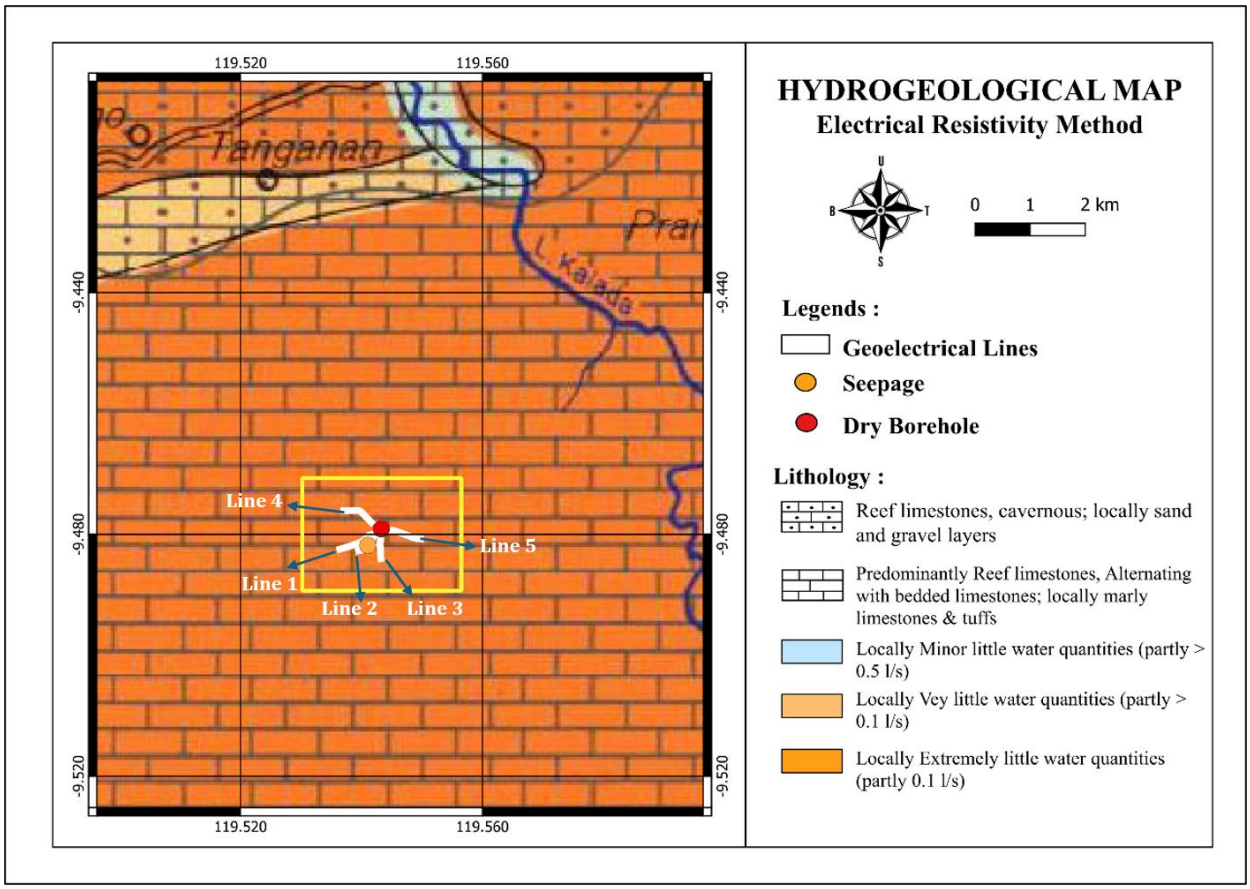


Figure 1. Hydrogeological Map of the study area showing the measurement location (yellow square) where the water quantities are extremely low (Meiser et al., 1965).

2. METHODS

The electrical resistivity method is a method in the field of geophysics that studies the electrical properties within the earth (Wahid et al., 2022). ERT has become a reliable geophysical method in various ways, it has the characteristics of large amounts of data acquisition, low cost, and easy interpretation. 2D inversion data verify that the resistivity model retrieved by the electrical resistivity not only evaluate the depth of lithology, but also the continuity and existence of the ground water potential (Wu et al., 2023). The principle of the resistivity geoelectric method involves injecting an electric current into the ground and then measuring the potential difference generated by that current injection, so that the resistivity value can be determined. Mathematically, this can be expressed as Equation 1.

$$\rho a = k \frac{\Delta V}{I} \tag{1}$$

Equation 2. determines the geometric factor k for the Dipole-dipole configuration.

$$k = \pi n a\,(n+1)(n+2) \tag{2}$$

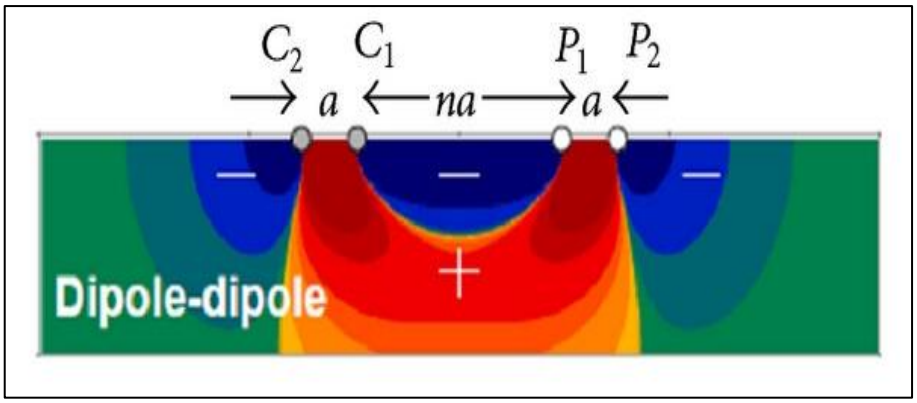


Figure 2. Dipole-dipole Electrode Configuration (Okpoli, 2013).

According to a study conducted by Neyamadpour et al., (2010), the Dipole-Dipole configuration provides better horizontal data coverage and produces a greater lateral extent of subsurface features, which is essential for identifying fracture-controlled groundwater pathways in carbonate formations. As shown in **Figure 2.** C1 and C2 serve as the current electrodes that inject electrical current into the ground, while P1 and P2 act as the potential electrodes that measure the resulting voltage difference at a separation distance of na from the current dipole, where n is the dipole separation factor and a is the electrode spacing. Furthermore, this configuration is well-suited for 2D resistivity surveys as it allows for a more detailed imaging of lateral subsurface variations compared to other electrode configurations (Dahlin & Zhou, 2004; Okpoli, 2013).

As shown in **Figure 3.** The search begins with literature review, such as regional geological map or hydrogeological map for reference, following the secondary data and elevation data (DEMNAS). Secondary data were obtained from the Center for Groundwater and Environmental Geology (PATGTL). Data acquisition was carried out from September 13th to 16th 2025, using a Dipole-dipole configuration with IRIS Resistivity Meter, an electrode spacing of a = 10 m. A total of five measurement lines were conducted, with lines 1 through 4 each spacing 620 m in length. Meanwhile, line 5 had a length of 880 m. From the field data acquisition, the values of voltage and current were obtained, which were then calculated using the dipole-dipole geometric factor to derive the apparent resistivity value (ρa). Before proceeding to the inversion stage, the elevation data obtained from DEMNAS was first incorporated into the .dat file to ensure topographic correction is applied during processing. The data then undergoes a quality control process through the elimination of bad datum points, once the data passes the quality check, the inversion process is carried out with 5 times iteration to optimize the results.

The inversion process employs the Least-Squares Inversion method, which applies the finite element approach to produce a model with smooth resistivity variations, and produces a 2D true resistivity cross-section with elevation (Loke & Barker, 1996). Along with the previous study, regional geological and hydrogeological maps, then incorporated into the interpretation stage to provide a comprehensive understanding of the subsurface conditions.

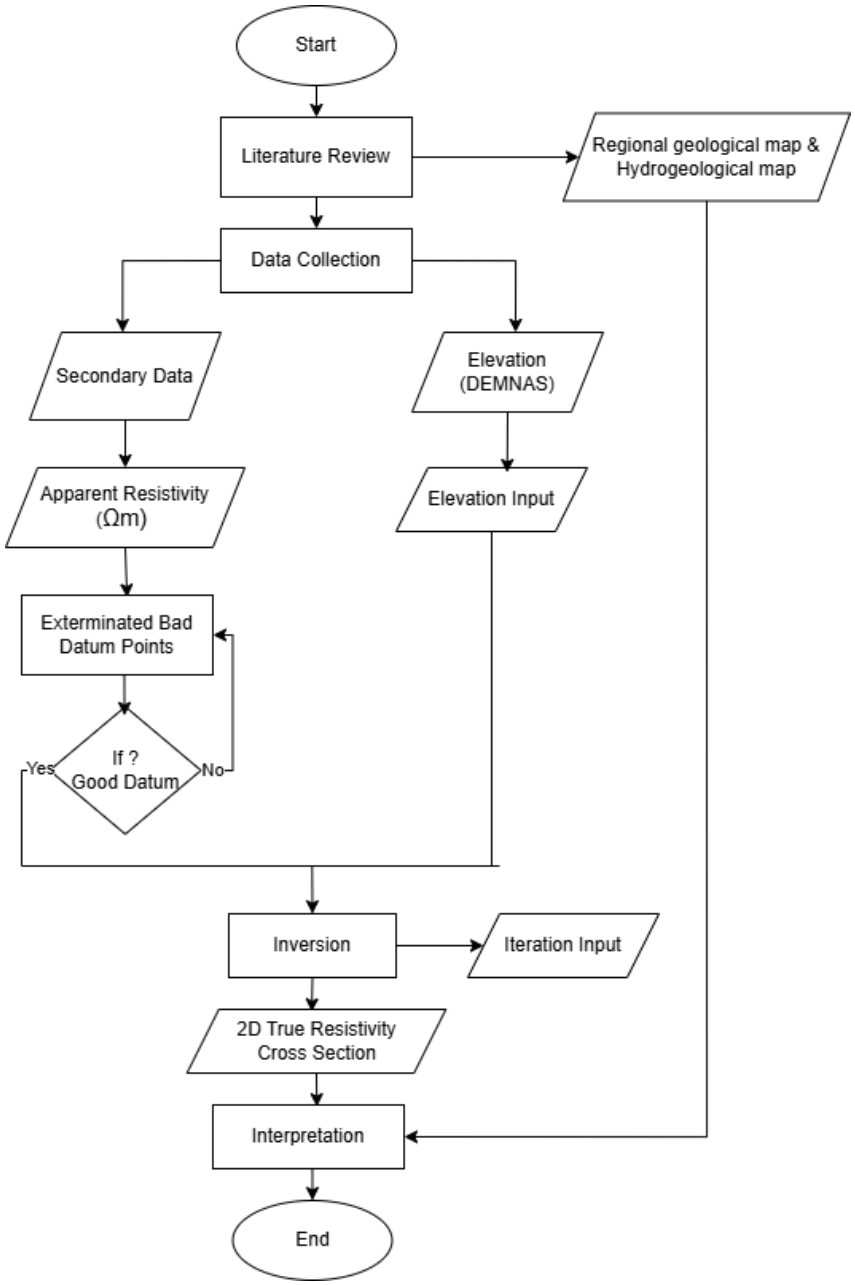


Figure 3. Data Processing Flowchart

Figure 4. also shows the location of the survey lines on the regional geological map. Lines 1 through 3 traverse two different formations, namely the Waikabubak and Pamalar Formations. The Waikabubak Formation, which consists of limestone with marl interbeds, and the Pamalar Formation, dominated by limestone and clay, give this area a varied hydrogeological character. Meanwhile, Lines 4 and 5 are located entirely within the Waikabubak Formation. In Line 2, groundwater seepage was observed, which is utilized by the local community as a source of clean water, although the discharge is relatively small. As for Line 5, a borehole was drilled in an attempt to locate groundwater, but no water was found, resulting in a dry borehole.

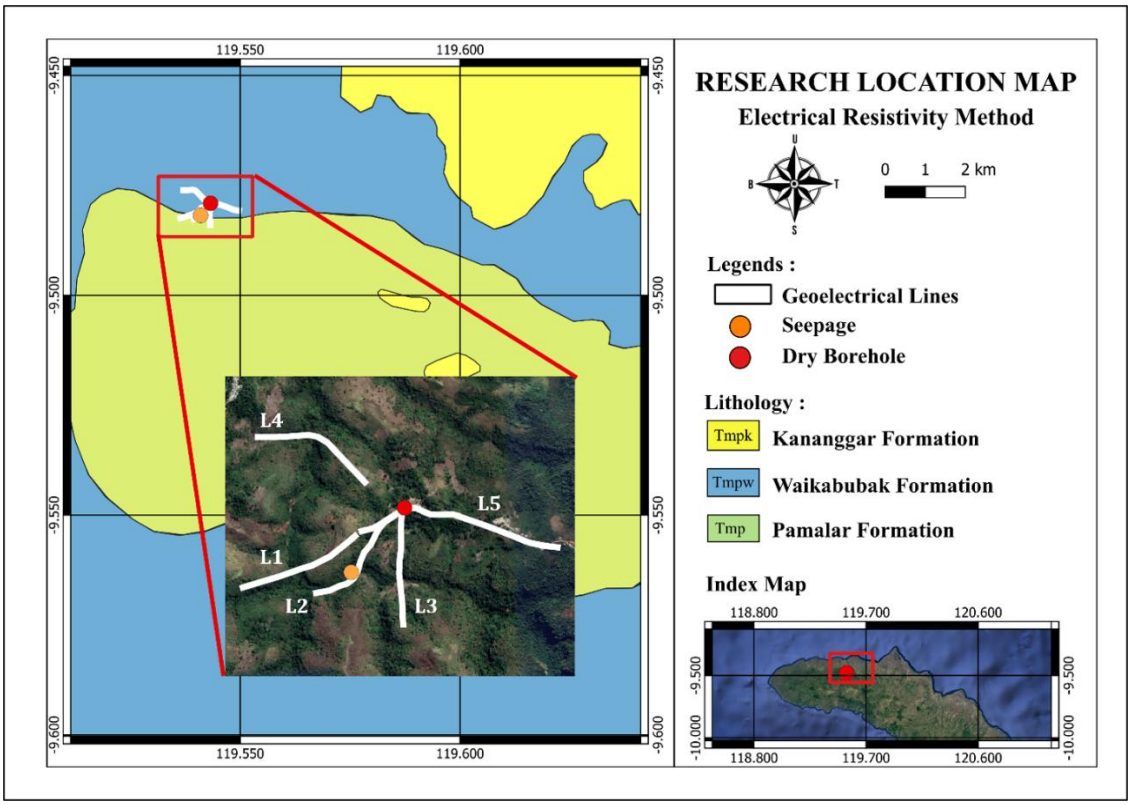


Figure 4. Research Location Map Showing the Geological map and the line orientation (Effendi & Apandi, 1993).

3. RESULT AND DISCUSSION

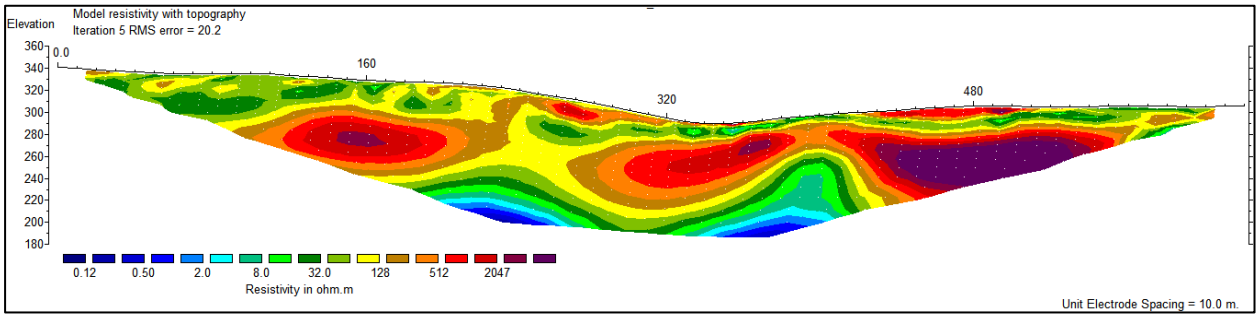
The inversion models from five lines show high RMS errors ranging from 17.7 to 24.8%. It needs to be addressed, as these values are higher than the commonly accepted (5-10 %) for resistivity inversion. This elevated error is attributed to several compounding factors, the extreme karst topography of the study area, the high electrode contact resistance encountered on the dry compact limestone surface, which degraded current injection and contributed to anomalously extreme apparent resistivity readings (Revil et al., 2017), and the resulting wide resistivity range of the dataset itself (<2.0 – > 128.0 Ωm), which is difficult to reproduce by the smoothness-constrained least-squares inversion algorithm that inherently assumes gradual resistivity variation between model cells rather than the sharp lithological contrasts present in the subsurface

Interpretation of the resistivity cross-sections was conducted by referring to standard resistivity values for geological materials (Telford et al., 1990) as well as previous studies conducted in geologically similar areas (Fillaily, 2009; Krisnasiwi, 2021). This approach allows for a more reliable correlation between resistivity anomalies and subsurface lithological variations. The resistivity value ranges and their corresponding lithological interpretations, along with the associated rock patterns, are presented in Tabel 1.

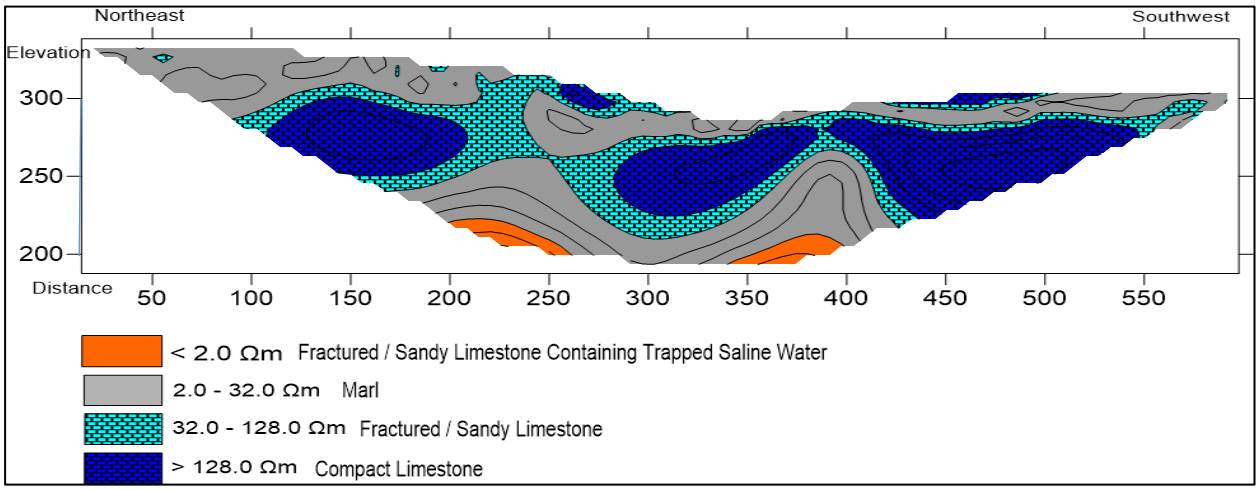
Tabel 1. Interpretation of Resistivity Value Based on The Previous Study (Federal Geographic Data Committee, 2006; Fillaily, 2009; Telford et al., 1990)

Resistivity Values	Constituent Rocks	Rock Patterns
< 2.0	Saline Water-Bearing Fractured Limestone	
2.0 – 32.0	Marl	
32.0 – 128.0	Fractured/Sandy Limestone	
>128	Compact Limestone	

The resistivity cross-section is the result of the inversion process that represents the actual subsurface resistivity distribution at the study area. Electrical conductivity in subsurface formations is strongly influenced by pore fluid conductivity, porosity, and moisture content, meaning that rocks with higher fracture density and water saturation tend to exhibit lower resistivity values. The marl layer, characterized by resistivity values of 2.0–32.0 Ωm and consisting of a mixture of clay and carbonate materials, exhibits relatively low resistivity due to the conductive nature of clay minerals and their capacity to retain significant amounts of water within their pore spaces, which enhances the overall electrical conductivity of the layer (Leroy et al., 2025; Marere et al., 2023). The fractured or sandy limestone layer with resistivity values 32.0-128.0 Ωm, exhibits moderate resistivity due to the presence of interconnected pore spaces and fractures that allow groundwater to accumulate and flow. Medium resistivity values in fractured limestone suggest the presence of moisture zones within the rock, where interconnected fractures facilitate groundwater storage and movement (Takele et al., 2025). In contrast, the compact limestone layer exhibits significantly higher resistivity values (>128.0 Ωm), as it lacks the pore spaces and fractures necessary to retain water. Consequently, compact limestone, which is dense and impermeable, produces high resistivity responses due to the absence of water as a conductive medium (Takele et al., 2025).



(a)



(b)

Figure 5. 2D Model of Line 1 Showing (a) Resistivity Model (b) Geological Interpretation

The first survey line, oriented in the northeast–southwest direction, was processed through an inversion with 5 iterations, yielding an error value of 20.2%. The resistivity values obtained from the inversion model of Line 1 range from 0.12 to 2047 Ωm. High resistivity values (>128 Ωm) are interpreted as compact limestone layers that not continuously distributed, but sufficiently dominant and extend toward the southwestern part of the cross-section, while intermediate resistivity values (32.0–128.0 Ωm) are interpreted as fractured or sandy limestone. The fractured/sandy limestone layer is distributed discontinuously along the survey line, appearing locally at depths of approximately 0 to 50 m, suggesting that this layer does not form a laterally continuous aquifer but rather occurs as isolated pockets of permeable zones. At the base of the cross-section, relatively low

resistivity values of approximately < 2.0 Ωm were recorded, which are interpreted as sandy limestone containing trapped saline water. This is supported by a previous study stating that a resistivity value of 0.2 Ωm indicates the presence of seawater (Satriani et al., 2012). Above this layer, a marl layer is identified, consisting of a mixture of clay and carbonate materials, with a resistivity range of 2.0 to 32.0 Ωm.

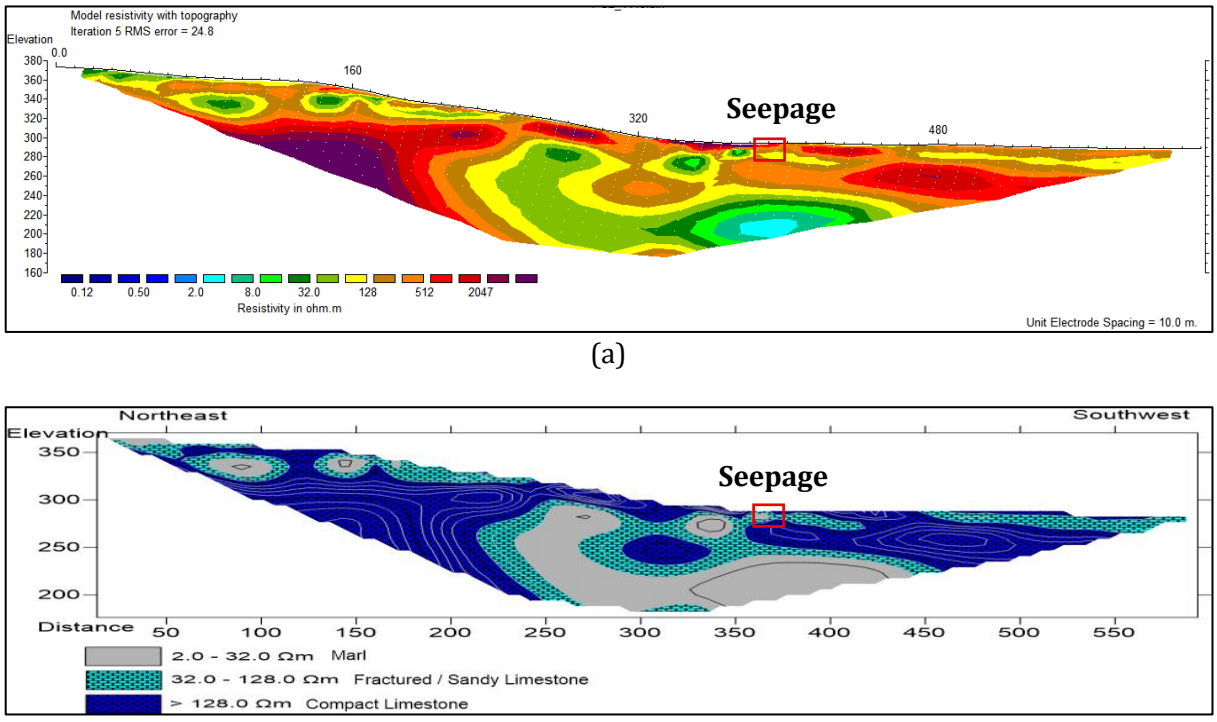
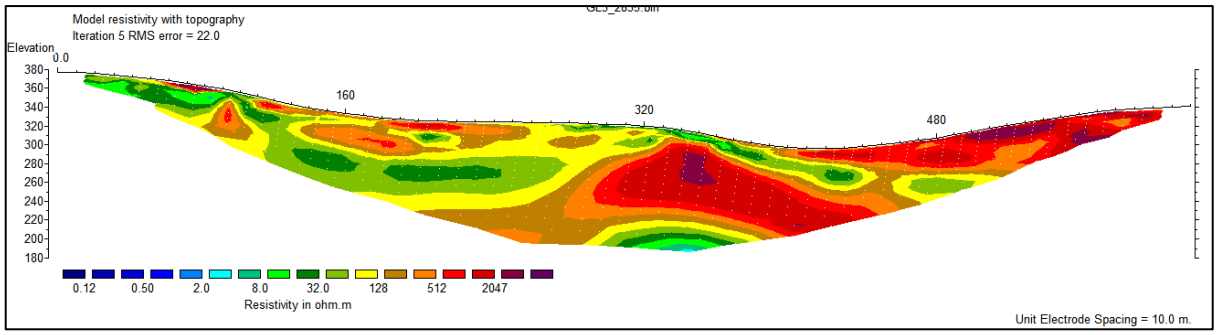
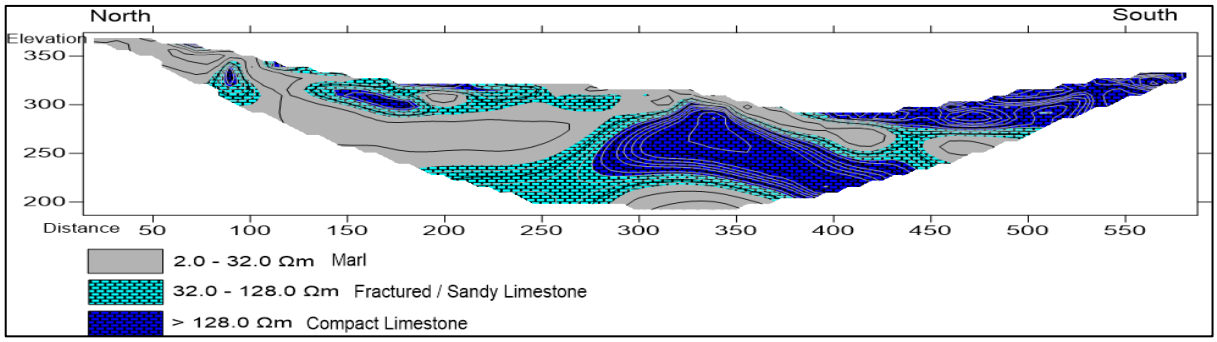


Figure 6. 2D Model of Line 2 Showing (a) Resistivity Model (b) Geological Interpretation

In Line 2, which runs in the northeast–southwest direction, the inversion results yielded an RMS error of 24.8%. The resistivity cross-section is dominated by high resistivity values (>128 Ωm), interpreted as compact limestone. Unlike Line 1, the compact limestone in this survey line appears more laterally continuous and extends to the surface. This suggests that the near-surface lithology along Line 2 is predominantly composed of hard, dense limestone with limited porosity. Intermediate resistivity values (32.0–128.0 Ωm), interpreted as fractured or sandy limestone, are distributed discontinuously along the survey line, appearing locally rather than forming a continuous layer. It is within these localized fractured/sandy limestone zones that groundwater seepage was identified. The seepage occurs where groundwater flows through the fractures of the limestone and its movement is impeded upon reaching the underlying marl layer, causing the water to discharge to the surface. This groundwater appears in the form of seepage or springs, making it difficult to identify exploitable locations (Inamoto & Sayama, 1993). Furthermore, the discharge from this seepage zone is considerably small, rendering it insufficient to serve as a reliable water source for the local community. The marl layer is identified beneath the seepage zone at depths ranging from approximately 20 to 82 m. The presence of this impermeable layer acts as a barrier to vertical groundwater movement, which explains the lateral discharge observed as surface seepage along this line.



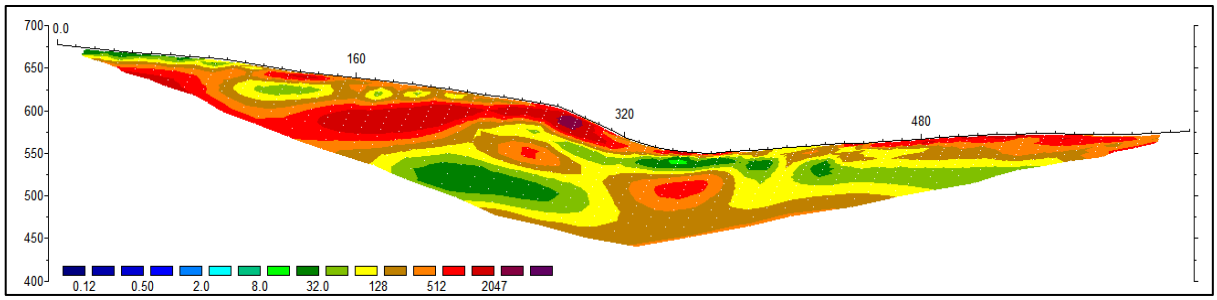
(a)



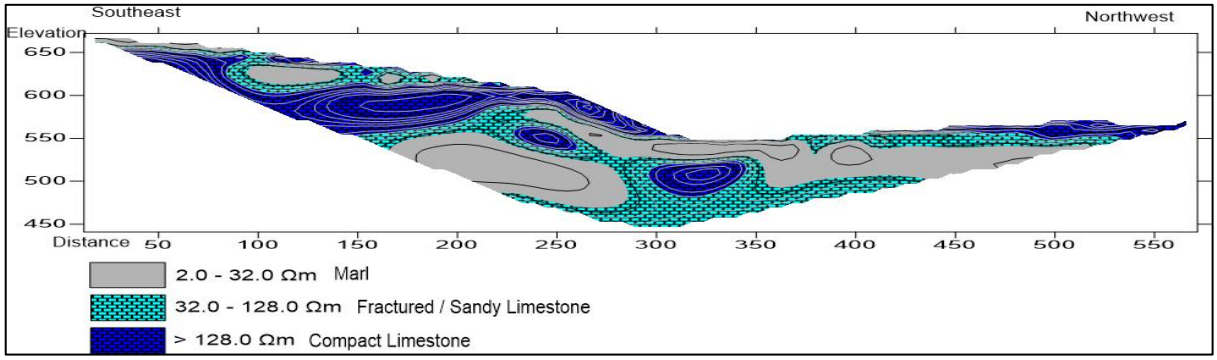
(b)

Figure 7. 2D Model of Line 3 Showing (a) Resistivity Model (b) Geological Interpretation

The third survey line, oriented in the North–South direction, produced an inversion model with an RMS Error of 22%. Resistivity values ranging from 32.0 to >128.0 Ωm appear to dominate the cross-section, interpreted as fractured to compact limestone. On the southern side of the cross-section, compact limestone extends to the surface. The marl layer (2.0–32.0 Ωm), characterized by low resistivity values, is appearing as a laterally continuous layer extending throughout the central portion of the survey line.



(a)



(b)

Figure 8. 2D Model of Line 4 Showing (a) Resistivity Model (b) Geological Interpretation

Line 4, which runs in the southeast–northwest direction, processed through 5 iterations with an RMS Error of 17.7%, is dominated by intermediate resistivity values ranging from 32.0 to 128.0 Ωm, interpreted as fractured or sandy limestone. These zones are considered moist or partially saturated, but do not represent significant groundwater storage. High resistivity values (>128 Ωm) distributed throughout the cross-section are interpreted as compact limestone layers. The compact limestone in this survey line appears to be discontinuously distributed, occurring locally rather than forming a laterally continuous layer. Notably, toward the central part of the cross-section, compact limestone is observed to outcrop at the surface.

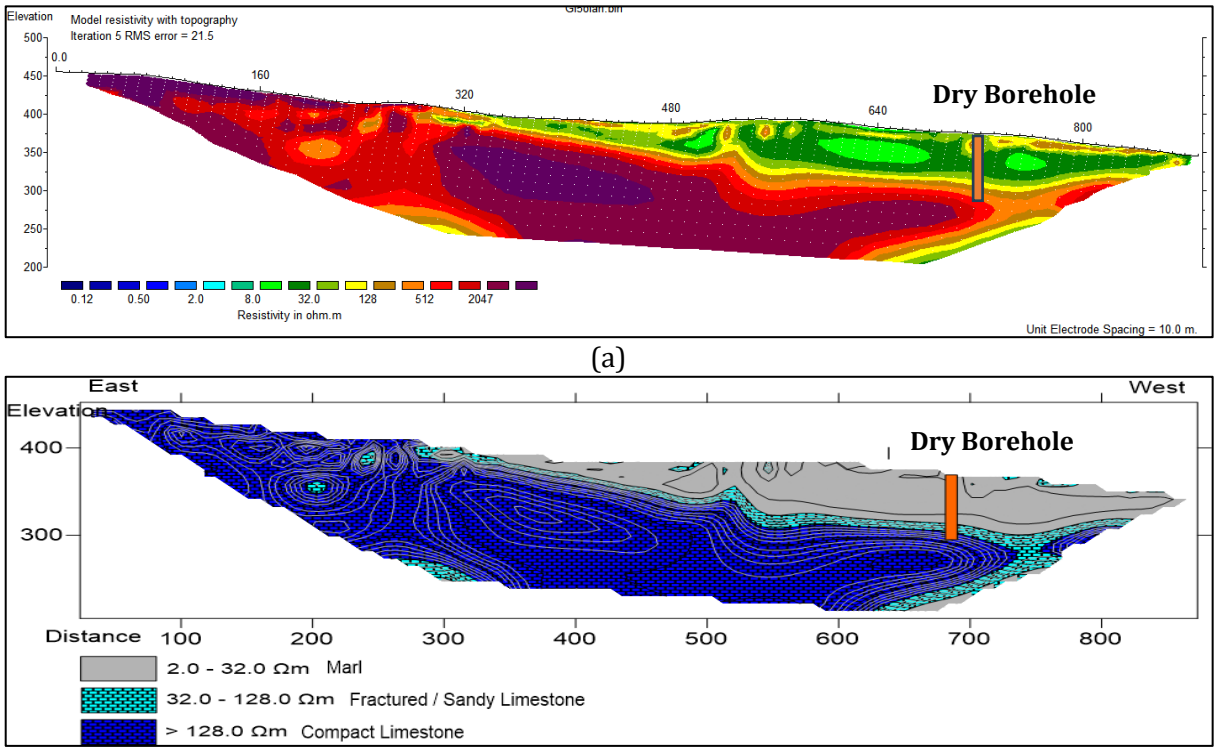


Figure 9. 2D Model of Line 5 Showing (a) Resistivity Model (b) Geological Interpretation

Line 5 extends in the east–west direction with a total length of 880 m. The inversion results show resistivity values ranging from 0.12 to 2047 Ωm with an RMS error of 21.5%. The cross-section is dominated by high resistivity values (>128 Ωm), interpreted as compact limestone, which appears as a thick and continuous layer extending toward the western part of the cross-section.

At the borehole location, situated at approximately 67 m, the subsurface sequence reveals a thick marl layer characterized by resistivity values of 2.0–32.0 Ωm, composed of a mixture of clay and carbonate materials with very low permeability. Above and within this marl sequence, a thin intercalation of fractured or sandy limestone is identified, exhibiting intermediate resistivity values of 32.0–128.0 Ωm. However, this fractured limestone layer is insufficiently thick to store or transmit groundwater in significant quantities. Beneath this sequence, the borehole penetrates into compact limestone (>128 Ωm), which acts as an aquifuge, an impermeable rock unit that neither stores nor transmits groundwater. The combination of thick marl overlying compact limestone, with only a thin and discontinuous fractured limestone intercalation, explains the dry borehole condition encountered at this location, as no productive aquifer zone was intersected during drilling.

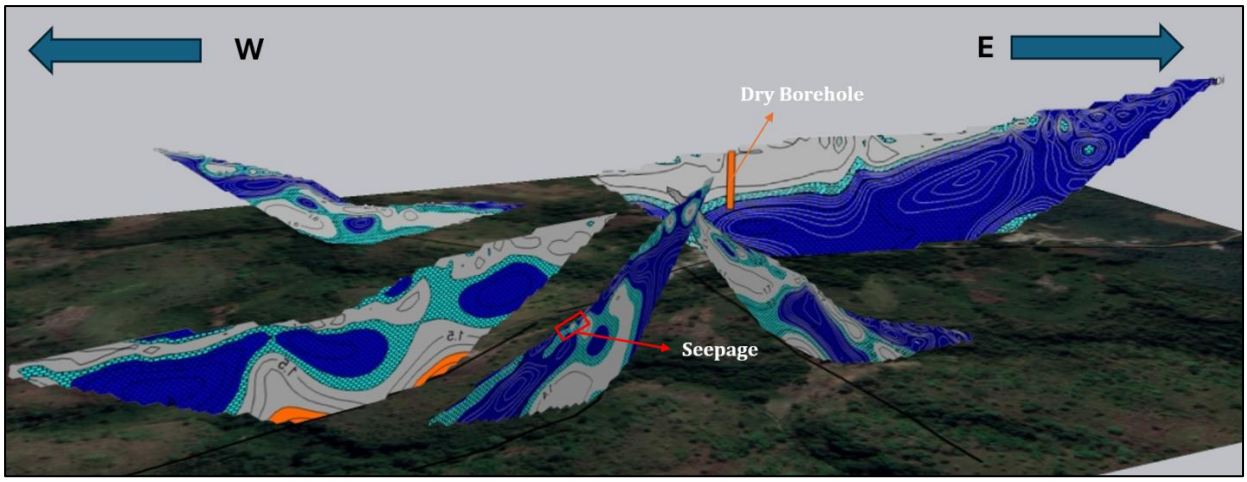


Figure 10. 3D Visualization Showing All the Lines in the Study Area

Based on **Figure 10.** generally, the interpretation results from all survey lines indicate that the Poguwatu Village area is predominantly underlain by compact limestone (>128 Ωm), which exhibits very low porosity and permeability. These rock characteristics cause it to function as an aquifuge, a rock layer that is neither capable of storing nor transmitting groundwater in any significant amount. This condition suggests that the aquifer potential in the study area is considerably limited and cannot be relied upon as an adequate source of clean water.

This is further supported by the findings observed in Line 2, where the groundwater seepage zone yielded only a very small discharge, characterized merely as moisture with insufficient water accumulation to full daily needs. A similar condition is also reflected by the dry borehole encountered in Line 5, which failed to yield any groundwater, further confirming the minimal groundwater potential across the study area.

Therefore, based on the resistivity analysis conducted throughout all survey lines, it can be concluded that Poguwatu Village does not possess sufficient groundwater potential to meet the clean water demands of the local community. Consequently, further investigation into alternative water sources from surrounding areas is strongly recommended as a long-term solution to address the clean water needs of the Poguwatu Village community.

It is important to note that the subsurface interpretation presented in this study is based solely on resistivity values obtained from the 2D geoelectric measurements. In the absence of supporting data such as borehole logs, well data, or geochemical analysis, the lithological classification relies on reference resistivity ranges from the literature and regional geological context. Therefore, the interpreted rock units and groundwater potential zones should be considered as qualitative estimates, and further verification through direct to confirm the subsurface conditions.

4. CONCLUSION

This study confirms that 2D resistivity imaging using the Dipole-dipole configuration is capable of characterizing subsurface lithological variations in Poguwatu Village and identifying four lithological units based on resistivity distribution. Across the five survey lines, indicates that groundwater occurrence is associated with fractured or sandy limestone layers (32.0 – 128.0 Ωm), as evidenced by the seepage identified on Line 2. In contrast, compact limestone dominates much of the study area and acts as an aquifuge, preventing the storage and flow of groundwater, as demonstrated by the dry borehole encountered on Line 5.

These findings carry broader scientific implications for understanding groundwater occurrence in tropical karst terrains, where aquifer potential is governed less by bulk lithology than by the spatial distribution of localized fracture and pathways within an otherwise impermeable matrix. The relatively high RMS errors obtained across all survey lines further suggest that the Dipole-dipole configuration's geometric factor k is particularly sensitive to noise under dry, topographically rugged carbonate conditions, a consideration relevant to survey design in similar karst settings elsewhere.

Several methodological directions are recommended for future research. Integrating Vertical Electrical Sounding or Induced Polarization surveys at finer electrode spacing could help resolve the resistivity ambiguity. In light of the limited groundwater potential identified across Poguwatu Village, further investigation into alternative water sources from surrounding areas is strongly recommended as a long-term solution to fulfill the clean water needs of the local community.

ACKNOWLEDGEMENTS

The authors would like to express their gratitude to the Center for Groundwater and Environmental Geology (PATGTL), particularly the Laboratory and Technical Facilities Team, for providing the secondary data used in this study. Appreciation is also extended to all parties who have contributed, both technically and administratively, to the completion of this research and the writing of this article.

REFERENCES

Badan Meteorologi, K. dan G. (2021). *Peta Rata-Rata Curah Hujan dan Hari Hujan Periode 1991-2020 Indonesia*.

Badan Pusat Statistik Kabupaten Sumba Barat. (2025). *Kabupaten Sumba Tengah Dalam Angka 2025*. BPS Statistics of Sumba Barat Regency.

Dahlin, T., & Zhou, B. (2004). A numerical comparison of 2D resistivity imaging with 10 electrode arrays. *Geophysical Prospecting*, *52*(5), 379–398. https://doi.org/10.1111/j.1365-2478.2004.00423.x

Effendi, A. C., & Apandi, T. (1993). *Geological Map of the Waikabubak and Waingapu (Scale 1:250.000)*. Pusat Penelitian dan Pengembangan Geologi.

Federal Geographic Data Committee. (2006). *FGDC Digital Cartographic Standard for Geologic Map Symbolization Reston, Va., Federal Geographic Data Committee Document Number FGDC-STD-013-2006*. https://pubs.usgs.gov/tm/2006/11A02/FGDCgeostdTM11A2_web_all.pdf

Fillaily, A. (2009). *Pendugaan Kedalaman Zona Akuifer Dengan Menggunakan Metode Geolistrik Konfigurasi Schlumberger di Desa Lukumihi, Kec. Kanatang, Kab. Sumba Timur NUsa Tenggara Timur*. Universitas Brawijaya.

Firdaus, R., Widyaningrum, Y., & Inriawati, A. (2023). Identifikasi lapisan akuifer menggunakan metode geolistrik resistivitas konfigurasi dipole-dipole di Kelurahan Padang Mulya Kecamatan Koba. *Jurnal Riset Fisika Indonesia*, *4*(1), 17–24. https://doi.org/10.33019/jrfi.v4i1.4314

Hartmann, A., & Baker, A. (2017). Modelling karst vadose zone hydrology and its relevance for paleoclimate reconstruction. *Earth-Science Reviews*, *172*(August), 178–192. https://doi.org/10.1016/j.earscirev.2017.08.001

Hartmann, A., Goldscheider, N., Wagener, T., Lange, J., & Weiler, M. (2014). Karst water resources in a changing world: Review of hydrological modeling approaches. *Reviews of Geophysics*, *52*, 218–242. https://doi.org/10.1002/2013RG000443

Hussein, M. A., Ali, M. Y., & Hussein, H. A. (2023). Groundwater Investigation through Electrical Resistivity Tomography in the Galhareri District, Galgaduud Region, Somalia: Insights into Hydrogeological Properties. *Water (Switzerland)*, *15*(18). https://doi.org/10.3390/w15183317

Inamoto, A., & Sayama, M. (1993). Hydrogeology of Sumba Island, Nusa Tenggara Timur, Indonesia. *Journal of the Japan Society of Engineering Geology*, *34*(4), 178–193. https://doi.org/10.5110/jjseg.34.178

Krisnasiwi, I. F. (2021). Pendugaan potensi air tanah menggunakan metode geolistrik di Kecamatan Righu Kabupaten Sumba Barat Propinsi Nusa Tenggara Timur. *Jurnal Ilmiah Teknologi FST Undana*, *15*(1), 53–58. https://ejurnal.undana.ac.id/index.php/jurnal_teknologi/article/view/4318/2652

Leroy, P., Maineult, A., Mendieta, A., & Jougnot, D. (2025). A mechanistic model for the complex conductivity of clay materials. I. Theory. *Geophysical Journal International*, *241*(1), 86–109. https://doi.org/10.1093/gji/ggae411

Loke, M. H., & Barker, R. D. (1996). Rapid least-squares inversion of apparent resistivity

pseudosections by a quasi-Newton method. *Geophysical Prospecting*, *44*(1), 131–152. https://doi.org/10.1111/j.1365-2478.1996.tb00142.x

Marere, O S; Dio, & E; Iwhiwhu. (2023). Electrical Resistivity Tomography and Vertical Sounding for Groundwater Potentials in Erhoike Community. *J. Appl. Sci. Environ. Manage*, *27*(6), 1189–1192. https://dx.doi.org/10.4314/jasem.v27i6.19

Meiser, P., Pfeiffer, D., Purbohadiwidjojo, M., & Sukardi. (1965). *Hydrogeological Map of the Isle of Sumba (Scale 1:250000)*. Direktorat Geologi.

Multi, W., Kotarumalos, S. H., & Limehuwey, R. (2023). Pendugaan lapisan akuifer menggunakan metode geolistrik di Maluku Tengah. *Jurnal Geosains*, *1*(1), 1–9. https://doi.org/10.30598/tanahgoyang.1.1.1-9

Neyamadpour, A., Wan Abdullah, W. A. T., Taib, S., & Neyamadpour, B. (2010). Comparison of Wenner and dipole-dipole arrays in the study of an underground three-dimensional cavity. *Journal of Geophysics and Engineering*, *7*(1), 30–40. https://doi.org/10.1088/1742-2132/7/1/003

Okpoli, C. C. (2013). Sensitivity and resolution capacity of electrode configurations. *International Journal of Geophysics*, *2013*(Dic). https://doi.org/10.1155/2013/608037

Prabawa, S. E., Iswahyudi, A., & Warnana, D. D. (2020). Pendugaan Potensi Air Tanah Di Daerah Sumba Timur Dengan Menggunakan Data Citra Satelit dan Geolistrik. *Jurnal Geodesi Dan Geomatika*, *3*(2), 135–142. https://doi.org/10.14710/elipsoida.2020.9203

Revil, A., Coperey, A., Shao, Z., Florsch, N., Fabricius, I. L., Deng, Y., Delsman, J. R., Pauw, P. S., Karaoulis, M., de Louw, P. G. B., van Baaren, E. S., Dabekaussen, W., Menkovic, A., & Gunnink, J. L. (2017). Complex conductivity of soils. *Water Resources Research*, *53*(8), 7121–7147. https://doi.org/10.1002/2017WR020655

Satriani, A., Loperte, A., Imbrenda, V., & Lapenna, V. (2012). Geoelectrical surveys for characterization of the coastal saltwater intrusion in metapontum forest reserve (Southern Italy). *International Journal of Geophysics*, *2012*. https://doi.org/10.1155/2012/238478

Stevanović, Z. (2019). Karst waters in potable water supply: a global scale overview. *Environmental Earth Sciences*, *78*(23), 1–12. https://doi.org/10.1007/s12665-019-8670-9

Takele, T., Husein, M., Diriba, D., & Assefa, G. (2025). Application of electrical resistivity tomography for groundwater evaluation in Yirgacheffe Town and its environs, Main Ethiopian Rift. *HydroResearch*, *8*, 202–208. https://doi.org/10.1016/j.hydres.2024.11.003

Telford, W. M., Geldart, L. P., & Sheriff, R. E. (1990). *Applied Geophysics* (2nd ed.). Cambridge University Press.

Torrese, P. (2020). Investigating karst aquifers: Using pseudo 3-D electrical resistivity tomography to identify major karst features. *Journal of Hydrology*, *580*(August), 124257. https://doi.org/10.1016/j.jhydrol.2019.124257

Wahid, A., Sunaryo, Susilo, A., & Wiyon. (2022). Identification of karstification zoning and aquifer channels in Karst Basin at Sendang Biru Beach, Malang-Indonesia: A Case Study. *International Journal of Design and Nature and Ecodynamics*, *17*(3), 391–400. https://doi.org/10.18280/ijdne.170309

Wu, J., Dai, F., Liu, P., Huang, Z., & Meng, L. (2023). Application of the electrical resistivity tomography in groundwater detection on loess plateau. *Scientific Reports*, *13*(1), 1–15. https://doi.org/10.1038/s41598-023-31952-7